Nifuroxazide enhances radiotherapy efficacy against hepatocellular carcinoma by upregulating PD-L1 degradation via the ubiquitin-proteasome pathway

Abbreviated Title: Nifuroxazide prompts anti-tumor efficacy of RT

Author Names and Affiliations: Tiesuo Zhao[1,2,3]†, Pengkun Wei[1,2,4]†, Congli Zhang[1,2], Shijie Zhou[1,2], Shuoshuo Guo[1,2], Sichang Cheng[1,2], Zerui Gan[1,2], Yuanling Xia[1,2], Yongxi Zhang[5], Sheng Guo[1,2], Jiateng Zhong[2], Zishan Yang[1,2], Fei Tu[2], Qianqing Wang[6,7], Jin Bai[6,7], Feng Ren[3*], Zhiwei Feng[1,2*], Huijie Jia[2*]

[1]Department of Immunology, School of Basic Medical Sciences, Xinxiang Medical University, Xinxiang, Henan 453000, P.R.China.

[2]Xinxiang Engineering Technology Research Center of immune checkpoint drug for Liver-Intestinal Tumors, Xinxiang Medical University, Xinxiang, Henan 453000, P.R.China.

[3]Henan International Joint Laboratory of Immunity and Targeted Therapy for Liver-Intestinal Tumors, Xinxiang Medical University, Xinxiang, Henan 453000, P.R.China.

[4]Zhengzhou Central Hospital Affiliated to Zhengzhou University, Zhengzhou 450000, P.R.China.

[5]Department of Oncology, The Third Affiliated Hospital of Xinxiang Medical University, Xinxiang, Henan 453000, P.R.China.

[6]Department of Gynecology, Xinxiang Central Hospital, 453000, Xinxiang, Henan, P.R.China.

[7]The fourth clinical college, Xinxiang Medical University, Xinxiang, Henan 453000, P.R.China.

†Tiesuo Zhao and Pengkun Wei have contributed equally to this work

*Correspondence: 131010@xxmu.edu.cn; 123066@xxmu.edu.cn; renfeng@xxmu.edu.cn

Abstract

Background: Radiation therapy is a primary treatment for hepatocellular carcinoma (HCC), but its effectiveness can be diminished by various factors. The over-expression of PD-L1 has been identified as a critical reason for radiotherapy resistance. Previous studies have demonstrated that nifuroxazide exerts antitumor activity by damaging the Stat3 pathway, but its efficacy against PD-L1 has remained unclear. In this study, we investigated whether nifuroxazide could enhance the efficacy of radiotherapy in HCC by reducing PD-L1 expression.

Methods: This study investigated the effects of Nifuroxazide on hepatocellular carcinoma using HepG2 cells and female C57BL/6 mice. HepG2 cells were irradiated and treated with different concentrations of Nifuroxazide, and various parameters were evaluated. Female C57BL/6 mice were divided into four groups and a hepatocellular carcinoma model was established. Each group received different treatments and observations were recorded. Spleens and tumor tissues were isolated from the mice and analyzed for tumor cell proliferation, apoptosis, and lymphocyte protein expression. T-cell subsets and the percentage of NK cells in the spleens were determined using flow cytometry.

Results: Our results showed that nifuroxazide significantly increased the sensitivity of tumor cells to radiation therapy by inhibiting cell proliferation and migration while increasing apoptosis *in vitro*. Additionally, nifuroxazide attenuated the up-regulation of PD-L1 expression induced by irradiation, which may be associated with increased degradation of PD-L1 through the ubiquitination-proteasome pathway. Furthermore, nifuroxazide greatly enhanced the efficacy of radiation therapy in H22-bearing mice by inhibiting tumor growth, improving survival, boosting the activation of T lymphocytes, and decelerating the ratios of Treg cells in spleens. Importantly, nifuroxazide limited the increased expression of PD-L1 in tumor tissues induced by radiation therapy. This study confirms, for the first time, that nifuroxazide can augment PD-L1 degradation to improve the efficacy of radiation therapy in HCC-bearing mice.

Keywords: Nifuroxazide, radiotherapy, hepatocellular carcinoma, PD-L1

Introduction

Cancer continues to be the primary cause of death and a major public health issue globally [1]. Among the various types of cancer, hepatocellular carcinoma (HCC) has exhibited an increasing incidence and morbidity, and it is estimated that the number of new HCC cases will surpass one million by 2025 [2, 3]. The current therapeutic options for HCC comprise surgery, targeted therapy, radiation therapy, chemotherapy, and immunotherapy, among others. Nevertheless, most patients still experience an unfavorable prognosis. Consequently, the development of effective treatment strategies for HCC is a pressing and challenging issue [4].

Radiation therapy is a widely used localized therapeutic approach for the treatment of HCC [5, 6]. It has been demonstrated that radiation therapy can induce DNA damage and mutations in tumor cells through the generation of X-rays or γ-rays, leading to the death of malignant cells [7]. Despite significant progress in recent decades, the effectiveness of radiation therapy is limited by various factors. Studies have shown that radiation therapy can contribute to the formation of an immunosuppressive tumor microenvironment (TME) by promoting the infiltration of M2 macrophages, increasing the number of regulatory T cells, impairing the function of CD8+ T lymphocytes, and inducing the release of immunosuppressive cytokines [8]. Therefore, improving the immunosuppressive state of HCC may enhance the clinical efficacy of radiation therapy.

Programmed cell death 1 ligand 1 (PD-L1) is a transmembrane glycoprotein predominantly expressed on T lymphocytes, B lymphocytes, macrophages, and tumor cells. Upon binding with programmed cell death protein 1 (PD-1), PD-L1 generates inhibitory signals that suppress the proliferation of T lymphocytes and accumulation of antigen-specific T cells in lymph nodes [9-11]. Radiation therapy induces DNA damage and repair, activating and up-regulating PD-L1, and creating an immune-suppressive microenvironment, which is a major contributor to radiotherapy resistance of tumors [12, 13]. Furthermore, tumor-associated macrophages (TAMs) also take part in shaping the tumor microenvironment by expressing PD-L1. In mice with tumors, inhibition of the PD-1/PD-L1 pathway significantly stimulated the activation of macrophages [14, 15]. Similarly, in HCC, radiation therapy up-regulates the expression of PD-L1 via the IFN-γ-Stat3 signaling pathway [16]. Therefore, blocking the PD-1/PD-L1 pathway may be an effective systemic treatment for enhancing the efficacy of radiation therapy.

The PD-1/PD-L1 pathway blockade has been shown to provide satisfactory clinical benefits for most

tumor types [17]. However, the development and research of new drugs are time-consuming, costly, and uncertain [18], exploring the potential indications of old drugs has been endorsed by scholars [19]. Nifuroxazide, an antidiarrheal drug, has been demonstrated to significantly inhibit the activation of Signal Transducer and Activator of Transcription 3 (Stat3) and has also exhibited effects in promoting the death of multiple myeloma cells and inhibiting tumor growth. Importantly, treatment with nifuroxazide has shown low toxicity that does not damage peripheral blood mononuclear cells [20]. However, the relationship between nifuroxazide and the expression of PD-L1 remains unknown, as well as whether nifuroxazide can enhance the efficacy of radiation therapy in tumors by blocking the expression of PD-L1.

We have revealed that nifuroxazide exerts a significant effect on promoting the degradation of PD-L1 in HCC cells. Notably, administration of nifuroxazide led to a reduction in the expression of PD-L1 in mice, which in turn enhanced the sensitivity of radiation therapy in mice with HCC. This approach may offer a promising combination strategy to counteract the radio-resistance of HCC.

Materials and methods

Regents and cell lines

The Nifuroxazide used in this study was obtained from Sigma-Aldrich (USA). The HepG2 and H22 cell lines were donated by Prof. Li Zhang (Jilin University, Jilin China) and maintained at Xinxiang Key Laboratory of Tumor Vaccine and Immunotherapy, located at Xinxiang Medical University in Xinxiang, Henan (P.R. China).

Cell viability assay

HepG2 cells were cultured and seeded in 96-well plates (Corning, New York, NY) at a density of 1×10^4/well. After 15 hours of incubation, nifuroxazide with varying concentrations (0, 0.3125, 0.625, 1.25, 2.5, 5, 10, 20, 40 μg/mL) were added and co-incubated for 24 or 48 hours with or without radiotherapy treatment. After the incubation period, Cell Counting Kit-8 (CCK-8, Beyotime Institute of Biotechnology, Shanghai, China) reagents were added into each well and incubated for an additional 2 hours. The optical density (OD) was measured at 450 nm using a microplate reader (SpectraMax iD3, Molecmlar Devices).

Wound-Healing assay

HepG2 cells were cultured and subjected to radiotherapy, then seeded in six-well plates (Corning, New York, NY) at a density of 3.5×10^5 cells per well, followed by an incubation period of 15 hours. A scratch was created in the middle of each well using a pipette tip. Afterwards, the cells were co-cultured with varying concentrations of nifuroxazide (0, 0.625, 1.25, 2.5, 5 μg/mL) for a period of 24 or 48 hours. Subsequently, the width of the scratch was recorded and measured.

Colony formation

HepG2 cells were treated with or without radiotherapy and then plated at a density of 2×10^3 cells per well in six-well plates from Corning, New York, NY. After an incubation period of 15 hours, nifuroxazide was added at various concentrations (0, 0.625, 1.25, 2.5, 5 μg/mL). The culture medium was periodically replaced and cell masses became visible by the 10th day. Subsequently, the cell colonies were detected and recorded.

Transwell

HepG2 cells were treated with or without radiotherapy and then plated at a density of 1×10^5 cells per well in the upper chamber, while different concentrations of nifuroxazide (0, 0.625, 1.25, 2.5, 5 μg/mL) were added. Meanwhile, 500 μL of culture medium was added to the lower chamber. After a 24-hour

incubation period, the lower chambers were drained and stained with crystal violet for 40 minutes. The results were subsequently observed under a microscope (Nikon, Japan) after sealing with neutral resin.

RT-PCR

HepG2 cells, treated with or without radiotherapy, were seeded at a density of 3.5×10^5 cells per well in six-well plates from Corning, New York, NY, and incubated for 15 hours. Nifuroxazide was then added at varying concentrations (0, 0.625, 1.25, 2.5, 5 μg/mL) into each well. After a period of 24 or 48 hours, total RNA was extracted from the cells using the Trizol reagent, following the instructions. The gene expression of PD-L1 was subsequently detected using PCR. The PCR primers used were as follows: For GAPDH, Forward-sequence: AGAAGGCTGGGGCTCATTTG, and Reverse-sequence: AGGGGCCATCCACAGTCTTC. For PD-L1, Forward-sequence: GAGCGTGACAAGAGGAAGGAATGG, and Reverse-sequence: TTGAGGCATTGAGTGGAGGCAAAG.

Establishment of tumor model and therapeutic options

The female C57BL/6 mice were procured from Skbex Biotechnology in Henan, China. The animal studies were approved by the Ethics Committee of Xinxiang Medical University located in Xinxiang, China. H22 cells were subcutaneously injected into the right dorsal of the mice at a concentration of 2×10^6/100 μl. After 7 days, the mice were randomly assigned to one of five groups: the PBS group, Radiation therapy group, nifuroxazide group, Radiation therapy plus Nifuroxazide group. Seven days after the inoculation, the mice were anesthetized using 1% sodium pentobarbital and underwent radiation therapy at a dose of 4 Gy. The following day, nifuroxazide was intratumorally injected at a dose of 200 μg per mouse once a day. On the eighth day after the last treatment, relevant indicators were measured.

Western blot

Total proteins were extracted using RIPA lysate buffer (Beyotime Institute of Biotechnology, Shanghai, China) for western blot detection. Briefly, the proteins were separated via 10% sodium dodecyl sulfate–polyacrylamide gel electrophoresis (SDS–PAGE). Following electrophoresis, the proteins were transferred to polyvinylidene fluoride membrane (EMD Millipore, Billerica, MA, USA). The PVDF membranes were then incubated with a buffer of 5% nonfat dry milk for 2 hours at room temperature. After being washed, the membranes were incubated with the following primary antibodies overnight at

4 ℃: PD-L1 (1:1000, Bioworld), p-Stat3 (1:1000, CST), Stat3 (1:1000, Bioworld), cleaved-caspase 3 (1:1000, Bioworld), Pro-Caspase 3 (1:2000, Bioworld), MMP2 (1:1000, CST), Ki67 (1:1000, Bioworld), PCNA (1:1000, SANTA), GSK3β (1:2000, Abways), cyclin D1 (1:2000, SANTA), Bcl-2 (1:2000, Abways), Bax (1:2000, Abways), Cytochrome C (1:1000, Biopple), cleaved-caspase 9 (1:2000, Abways), Pro-Caspase 9 (1:2000, Abways), PARP (1:1000, CST), cleaved-PARP (1:1000, CST), and Tubulin (1:1000, Sigma). The membranes were then washed and incubated with secondary antibodies (ZSGB-BIO, 1:5000). Finally, specific protein bands were visible using enhanced chemiluminescence (Beyotime Institute of Biotechnology) and detected using the chemiluminescence imaging instrument (Fusion FX spectra, Vilber). The images were semi-quantified using Quantity One software (Version 4.62; Bio-Rad Laboratories, Inc., Hercules, CA, USA).

Hematoxylin and eosin (HE) staining

Tumor tissue waxes were utilized to prepare tissue sections with a thickness of 4 μm. Following dewaxing and dehydration, the sections were stained using haematoxylin-eosin (Beyotime Biotechnology, Shanghai, China). Subsequently, the sections were rinsed and dried, and the resulting images were observed utilizing a microscope (Nikon, Japan).

Immunohistochemistry (IHC)

Following preparation as previously described [21], the tissue sections were incubated with primary antibodies against Ki67 and cleaved-caspase3, both purchased from Cell Signaling Technology (USA), overnight at 4 ℃. Subsequently, the sections were washed and incubated with biotin-labeled secondary antibodies for 30 minutes. After the completion of the reaction, streptavidin labeled with horseradish peroxidase was added. After a 30-minute incubation, the sections were chromogenically stained using the DAB reagent. Finally, the results were recorded utilizing a digital scanner (3DHISTECH, Pannoramic MIDI, China).

Immunofluorescence (IF)

The tissue samples were incubated with primary antibodies (CD3, 1:100, OmnimAbs; CD4, 1:200, CST; CD8, 1:800, CST; Granzyme B, 1:200, Bioworld; CD86, 1:400, Novus; CD11b, 1:200, Abways; PD-L1, 1:200, Bioworld) overnight at 4 ℃. Subsequently, the samples were rinsed and exposed to secondary antibodies labeled with corresponding fluorescent markers (Abways). After incubating at room temperature for 30 minutes, the samples were stained with DAPI solution (Beyotime) and

incubated for 5 minutes at room temperature. Lastly, the samples were washed and sealed with anti-fluorescence quenching agent, and the images were captured using a confocal microscope (AR1+, Nikon).

TUNEL

The detection of cell apoptosis in tumor tissues was conducted via TUNEL assay in accordance with the instructions provided in the manual from Beyotime Biotechnology. In brief, tumor sections were exposed to TUNEL detection solution and incubated at 37 ℃ for 60 minutes. Following a wash step, the sections were incubated with an anti-fluorescence quenching agent. The resulting images were captured using a confocal microscope (AR1+, Nikon).

Flow Cytometry

Spleen cell suspensions were prepared and the removal of red blood cells was accomplished with the use of erythrocyte lysate solution (Beyotime Biotechnology). The concentration of cells was then adjusted to 1×10^7 cells/ml. Subsequently, 100 μL of cell suspension was separately incubated with CD3, CD4, CD8, CD25, Foxp3, NK1.1, and Granzyme B antibodies (Biolegend) for 30 minutes. The cells were then washed using PBS buffer, and the ratios of immune cells were assessed utilizing flow cytometry (Cyto FLEX, Beckman).

Statistical analysis

Measurement data are expressed as the mean ± SD of three independent experiments, obtained from three separate and independent experimental trials. Statistical analysis was conducted using SPSS version 19.0, developed by IBM Corporation. To test the variation among the multiple groups, a one-way ANOVA was carried out, and the survival rate was analyzed using the Kaplan-Meier method with a log-rank test. Results with P-values below 0.05 were deemed to be statistically significant.

Results

The administration of Nifuroxazide augmented the radiosensitivity in the treatment of HCC

The study initially evaluated the impact of Nifuroxazide on HCC radiosensitivity by assessing cell proliferation, migration, and apoptosis. Results from Fig. 1A showed a significant inhibition of cell proliferation after 24 hours of radiotherapy, which was further enhanced when combined with Nifuroxazide. Interestingly, after 48 hours of radiotherapy, there was no significant inhibition of cell proliferation, but co-treatment with Nifuroxazide at concentrations of 2.5, 5, 10, 20, and 40 μg/ml resulted in evident inhibition. The combination of Nifuroxazide and radiotherapy also significantly inhibited cell proliferation, as demonstrated by cell cloning results (Fig. 1B). Additionally, the wound-healing assay and transwell assay showed substantial hindrance of cell migration at both 24 and 48 hours after radiotherapy. The inhibition of cell migration was further enhanced when the cells were co-treated with Nifuroxazide and radiotherapy (Fig. 1C and D). The combined treatment also resulted in a more potent pro-apoptotic effect on the cells. Fig. 1E indicated that radiotherapy alone did not have a pro-apoptotic effect on HCC, but the combination of radiotherapy and Nifuroxazide at concentrations of 1.25, 2.5, and 5 μg/ml exhibited significant pro-apoptotic effects. These findings suggest that Nifuroxazide may serve as a promising candidate drug to improve the radiosensitivity of HCC treatment.

Nifuroxazide had a significant effect on the expression of proteins associated with cell proliferation and apoptosis

To investigate the underlying mechanism of Nifuroxazide's ability to enhance HCC radiosensitivity, the study analyzed the expression of proteins associated with proliferation and apoptosis in HCC cells. The oncogene Stat3, which plays a critical role in tumor development, was effectively inhibited by radiotherapy in cells. Moreover, Nifuroxazide, an inhibitor of Stat3, was able to suppress the activation of Stat3 in Hep G2 cells that had undergone radiotherapy, as demonstrated in Fig. 2A and B. The expressions of PCNA and Ki67, which are closely linked to cell proliferation, were reduced by radiotherapy. Furthermore, when administered in conjunction with Nifuroxazide, this inhibitory effect was even more pronounced, as depicted in Fig. 2C and D. The combination therapy also suppressed the expression of cyclin D1, a protein involved in the cell cycle, as shown in Fig. 2E. In addition, the study examined apoptotic proteins, as illustrated in Fig. 2F-N. Caspase 3 is the primary enzyme responsible for the cleavage of cells during apoptosis. The results showed that the expression of cleaved-caspase 3

(c-caspase 3) was significantly increased at 24 or 48 hours after radiotherapy. Furthermore, the combination of radiotherapy and nifuroxazide resulted in a more pronounced upregulation of c-caspase 3, indicating a significant increase in cell apoptosis in HCC. Apoptosis can be induced through various pathways, with the mitochondrial apoptosis pathway being the most important. The results showed that the combination of radiotherapy and nifuroxazide had a significant impact on the expression of Bax, Bcl-2, and cytochrome C. Specifically, the combination therapy inhibited the expression of Bcl-2, which led to the translocation of Bax to mitochondria and the release of cytochrome C into the cytoplasm. The release of cytochrome C subsequently activated caspase 9, another pro-apoptotic protein. These events indicate that radiotherapy in combination with nifuroxazide significantly enhances apoptosis in HCC. PARP is the substrate of caspases and plays a vital role in regulating apoptosis. The activation of PARP is considered an important indicator of cell apoptosis and caspase 3 activation. The results demonstrated that the combination therapy increased the expression of PARP, suggesting that it had significant capabilities in inducing apoptosis. Overall, these findings suggest that the combination of radiotherapy and nifuroxazide can inhibit proliferation and increase apoptosis in HCC by regulating different tumor-related proteins.

Radiotherapy in combination with nifuroxazide significantly inhibited the growth of tumors in tumor-bearing mice and prolonged their survival period

A tumor-bearing mice model was used to validate the anti-tumor effect of the combination treatment. The treatment protocol for the study is illustrated in Fig. 3A. Seven days after the final treatment, the tumors were extracted, and the size and weight of the tumors were measured. The results showed that both the radiation therapy and nifuroxazide treatment groups exhibited significant inhibition of tumor growth compared to the PBS group, as evidenced by smaller tumor size and weight. Moreover, the combination treatment group demonstrated even greater inhibition of tumor growth than either mono-treatment group (Fig. 3B and C). Notably, the combination treatment also significantly prolonged the survival of tumor-bearing mice, with three mice still surviving on the 60th day (Fig. 3D). Histological analysis using HE staining showed that the tumor cells in the PBS group had irregular shape, high nucleo-cytoplasmic ratio, significant increase in heterotypic nuclei, and more pleomorphism of nuclei. However, the histomorphology significantly improved after the treatment with nifuroxazide and radiation therapy (Fig. 3E). These findings indicated that nifuroxazide played a crucial role in enhancing the efficacy of radiotherapy for HCC.

The combination of radiotherapy and nifuroxazide showed a remarkable inhibition of cell proliferation and an increase in cell apoptosis in tumor tissues

To further elucidate the anti-tumor mechanism of combining radiotherapy with nifuroxazide, the expression of proteins related to proliferation and apoptosis was evaluated in tumor tissues of tumor-bearing mice. As showed in Fig. 4A-C, the combination therapy significantly suppressed the expression of Ki67 and PCNA in tumor tissues while promoting the activation of caspase3, indicating its efficacy in hindering tumor cell proliferation, and inducing apoptosis. Additionally, the TUNEL assay showed a marked increase in the apoptotic rate of tumor cells upon the combination therapy (Fig. 4D). Moreover, the levels of proteins involved in cell proliferation (p-Stat3, PCNA, Ki67, and cyclin D1) were analyzed in the tumor tissues. Fig. 4E-I revealed that the combination therapy strikingly reduced the levels of associated proteins, indicating its potential in suppressing tumor cell proliferation. Subsequently, the cell apoptosis in tumor tissues was evaluated, and the expression of pro-apoptotic proteins (c-caspase3, Bax, and Cytochrome C) was observed to be significantly upregulated in the tumor tissues of mice treated with radiotherapy plus nifuroxazide, whereas the expression of anti-apoptotic protein (BCL-2) was downregulated (Fig. 4J-N). These results suggest that the combination therapy of radiotherapy and nifuroxazide effectively inhibits tumor cell proliferation and induces apoptosis by regulating the expression of proteins related to proliferation and apoptosis.

The combination of radiotherapy and nifuroxazide significantly boosted the activation of tumor-infiltrating lymphocytes and increased the population of M1 macrophages in tumor bearing mice

The impact of combining radiotherapy with nifuroxazide was comprehensively elucidated by assessing the infiltration of lymphocytes and M1 macrophages in tumor tissues. As showed by Fig. 5A-E, the combination therapy significantly augmented the infiltration of $CD4^+$ and $CD8^+$ lymphocytes, and stimulated the activation of lymphocytes (Granzyme B^+). Additionally, it increased the polarization of M1 macrophages ($CD11^+CD86^+$) (Fig. 5A-E). Furthermore, the expression of associated proteins also demonstrated the same results (Fig. 5F-I). These findings indicate that the combination of radiotherapy and nifuroxazide can effectively enhance the anti-tumor immune response in mice with tumors.

3.6. Radiotherapy combined with nifuroxazide noticeably regulated the ratios of immune cells in the spleens

As the spleen is an essential immune organ, it plays a crucial role in the peripheral immune response.

To quantify the ratios of immune cells in different groups of tumor-bearing mice, flow cytometry was employed. The results showed that treatment with radiotherapy or nifuroxazide led to a substantial increase in the number of $CD8^+$ lymphocytes, activated lymphocytes (Granzyme B^+), and NK cells in the spleens of mice compared to the PBS group. Moreover, the combined treatment resulted in the highest number of these cells among all the groups (Fig. 6B, D and E). Additionally, the ratio of $CD4^+$ lymphocytes in the spleens of mice treated with radiotherapy did not show any difference when compared to the PBS group. However, the ratio was significantly increased when radiotherapy was combined with nifuroxazide (Fig. 6A). Furthermore, Treg cells are crucial immunosuppressive cells that facilitate the immune evasion of tumor cells. Our findings indicate that treatment with radiotherapy leads to a significant increase in the ratio of Treg cells (Fig. 6C). However, the trend could be reversed after administering nifuroxazide treatment, suggesting that nifuroxazide may enhance the antitumor effects of radiotherapy by regulating the immune response.

Nifuroxazide in combination with the radiotherapy significantly increased the degradation of PD-L1 through ubiquitin-proteasome pathway

PD-L1 is a co-inhibitory protein expressed by various cells, including tumor cells, and its pathway has been shown to inhibit the anti-tumor function of T lymphocytes. PD-L1 is considered a critical indicator of radiotherapy resistance. Therefore, we investigated whether nifuroxazide enhances radiosensitivity in HCC via the PD-1/PD-L1 pathway. Our results showed that radiotherapy significantly inhibited the expression of p-Stat3 (Fig. 2A, B), but induced the upregulation of PD-L1 expression, which was effectively reversed by combined treatment with nifuroxazide (Fig. 7A). These results suggest that nifuroxazide may be a potential PD-L1 inhibitor, but its effect is independent of the Stat3 pathway. Surprisingly, we found that radiotherapy also upregulated PD-L1 mRNA expression, which was not affected by nifuroxazide treatment (Fig. 7B). These results suggest that nifuroxazide cannot regulate PD-L1 gene expression. The proteasome pathway is a key pathway involved in protein degradation. Our findings demonstrate that the inhibitory effect of nifuroxazide on PD-L1 expression was counteracted by the proteasome inhibitor (Fig. 7C). Moreover, nifuroxazide treatment clearly increased the expression of GSK3β (Fig. 7D). Additionally, the inhibitor of GSK3β reversed the downregulation of PD-L1 expression in cells treated with nifuroxazide (Fig. 7E). These findings confirmed that nifuroxazide could increase the degradation of PD-L1 via the ubiquitin-proteasome pathway and ultimately restore the immunity of T lymphocytes (Fig. 7F).

The combination of Nifuroxazide and radiotherapy notably inhibited the expression of PD-L1 via the up-regulation of GSK3β expression

We next detected the expression level of PD-L1 in tumor tissues of HCC patients pre-and post-radiotherapy. The results showed a significant increase in PD-L1 expression in tumor tissues of HCC patients after radiotherapy, compared to pre-radiotherapy (Fig. 8A), which may account for the poor clinical response to radiotherapy. Similarly, we observed an elevation in PD-L1 expression in tumor tissues of mice receiving radiotherapy. However, treatment with Nifuroxazide effectively blocked the up-regulation of PD-L1 induced by radiotherapy (Fig. 8B and C). Notably, the study demonstrated that treatment with Nifuroxazide significantly increased the expression of GSK3β in mice, regardless of radiotherapy treatment (Fig. 8D). These findings suggest that Nifuroxazide may enhance the degradation of PD-L1 and improve the therapeutic response to radiotherapy.

Discussion

Radiation therapy is a crucial approach in the management of HCC, but its effectiveness is limited by radioresistance. Our investigation has confirmed that nifuroxazide can enhance the immune response against tumors induced by radiation therapy by promoting the degradation of PD-L1 in HCC. PD-L1 is predominantly expressed on the surface of tumor cells and severely obstructs the immune response against tumors by binding to PD-1. Several studies have indicated that overexpression of PD-L1 is a major cause of radioresistance [22-24]. Therefore, inhibition of PD-L1 may prove to be an effective strategy to strengthen the antitumor effect of radiation therapy. D-mannose has been reported to significantly enhance the effects of radiotherapy by promoting PD-L1 degradation in triple-negative breast tumors [25]. Stat3 plays a key role in tumor progression and also regulates PD-L1 expression [26]. Nifuroxazide, a drug used to treat diarrhea, has been withdrawn from clinical practice. However, Nelson et al. discovered that nifuroxazide can inhibit the Stat3 pathway and suppress the proliferation of multiple myeloma cells [20]. Our study showed that nifuroxazide significantly inhibited the protein expression of PD-L1. Further investigations demonstrated that radiation therapy upregulated the gene level of PD-L1, while nifuroxazide did not change the gene level *in vitro*. Intriguingly, nifuroxazide covertly promoted the expression of GSK3β in cells that have undergone radiography. Simultaneously, the protease inhibitor blocked the inhibitory effect on PD-L1 expression. This finding suggests that nifuroxazide modulates the PD-L1 pathway through the ubiquitin-proteasome pathway rather than the mRNA pathway.

Furthermore, the overexpression expression of PD-L1 hinders the antitumor immunity response by inhibiting T lymphocyte function and macrophage polarization [27, 28]. The activity of T lymphocytes is closely associated with tumor progression, but it can become dysregulated due to the interaction between PD-1 and PD-L1 [29, 30]. Blocking the PD-1 and PD-L1 pathway can reverse T cell exhaustion and enhance their ability to eliminate tumor cells [31]. In our study, treatment with nifuroxazide effectively boosted T cell activation, with a more pronounced effect observed in mice receiving radiation therapy. Radiation therapy has been shown to induce an immunogenic effect that promotes T lymphocyte infiltration into tumors [32], but it also induces PD-L1 expression, which impairs T lymphocyte function [33]. Under these circumstances, nifuroxazide significantly enhanced T lymphocyte activation in mice receiving radiation therapy by reducing PD-L1 expression.

Moreover, the upregulation of PD-L1 on the surface of macrophages has been found to promote the

reduction of M1 macrophage polarization, which is recruited by tumor cells, leading to the inhibition of antitumor immunity [14, 34]. Studies have indicated a distinct decline in M1 macrophages in tumor tissues of patients undergoing radiation therapy [35, 36]. Therefore, a crucial strategy to enhance the antitumor effect of radiation therapy is to reverse macrophage polarization. Our research confirmed that nifuroxazide had a positive effect on promoting M1 macrophage polarization. Notably, while radiation therapy suppressed the infiltration of M1 macrophages, the number of M1 macrophages significantly increased in tumor tissues of mice treated with nifuroxazide and radiation therapy. These findings demonstrate that nifuroxazide plays a vital role in strengthening the antitumor immunity of radiation therapy for HCC by reversing macrophage polarization.

Conclusions

To summarize, the antitumor effect of radiation therapy is impaired due to the induction of PD-L1 expression. High expression of PD-L1 hinders the antitumor function of T lymphocytes and macrophages. However, nifuroxazide significantly inhibits PD-L1 up-regulation induced by radiation therapy, enhances the activation of T lymphocytes and the ratio of M1 macrophages, and decreases the number of Treg cells (Fig. 9). We confirm that nifuroxazide improves the antitumor effect of radiotherapy and provides a synergistic therapeutic strategy for HCC patients, especially those who are radioresistant.

Funding

This study was financially supported by the Doctor Launch Fund of Xinxiang Medical University (grant nos. 505017, 502006 and 505016), and the Key Projects of Scientific Research for Higher Education of Henan Province (grant no. 21A310012), the Young Backbone Teacher Training Projects of Universities in Henan province (grant no. 2020GGJS149), the Science and Technology Research Project of Henan Province (grant no. 222102310016), the Major Science and Technology Project of Xinxiang City (ZD2020005), the Science and Technology Project of Xinxiang (GG2019043), the Medical Education Research Project of Henan Province (grant no. Wjlx2020305), the Teaching and Scientific Research Program of Basic Medical College, Xinxiang Medical University (grant no. JCYXYJX202006), the Graduate Student Innovation Support Plan (grant no. YJSCX202149Y), the Innovation and Entrepreneurship Training Programmed for college student (grant no. 202210472005).

Competing interests

The authors declare no competing financial interests.

Ethics approval and consent to participate

This study was performed in accordance with the national guidelines, and with the approval of the institution for the care and use of animals (IACUC) and Ethics Committee of Xinxiang Medical University (No. XYLL-20220117, Date: 2022/03/09, Xinxiang, China). Each participant signed the written informed consent form. These experiments were carried out in accordance with the ethical standards laid down in the 1964 Declaration of Helsinki and its later amendments.

Availability of data and material

All data needed to evaluate the conclusions in the paper are present in this article or the supplementary materials. All materials may be made available to the scientific community upon request.

Authors' contributions

Conceptualization: HJ, ZF, FR. Methodology: TZ, PW, CZ, SZ, SG, SC, ZG, YX. Investigation: TZ, PW, CZ, SZ, SG, SC, ZG, YX. Visualization: FT, QW, JB. Funding acquisition: TZ, FR, ZF, HJ, PW, SZ, YZ. Project administration: HJ, TZ, ZF, FR. Supervision: HJ. Writing – original draft: TZ, PW. Writing – review & editing: YZ, SG, JZ, ZY. All authors read and approved the final paper.

Acknowledgements

We especially thank Dr. Yinghua Ji of the The First Affiliated Hospital of Xinxiang Medical University for helpful criticism, discussion, and encouragement.

Consent for publication

Not applicable.

References

1. Siegel RL, Miller KD, Fuchs HE, Jemal A. Cancer Statistics, 2021. CA Cancer J Clin. 2021;71:7-33.

2. Feng RM, Zong YN, Cao SM, Xu RH. Current cancer situation in China: good or bad news from the 2018 Global Cancer Statistics? Cancer Commun (Lond). 2019;39:22.

3. Hepatocellular carcinoma. Nat Rev Dis Primers. 2021;7:7.

4. Jiri T, Igor K, Mba. Hepatocellular carcinoma future treatment options. Klin Onkol. 2020;33:26-29.

5. Klein J, Dawson LA. Hepatocellular carcinoma radiation therapy: review of evidence and future opportunities. Int J Radiat Oncol Biol Phys. 2013;87:22-32.

6. Chen B, Wu JX, Cheng SH, Wang LM, Rong WQ, Wu F, et al. Phase 2 Study of Adjuvant Radiotherapy Following Narrow-Margin Hepatectomy in Patients With HCC. Hepatology. 2021;74:2595-2604.

7. Barber GN. STING: infection, inflammation and cancer. Nature reviews. Immunology. 2015;15:760-770.

8. Shevtsov M, Sato H, Multhoff G, Shibata A. Novel Approaches to Improve the Efficacy of Immuno-Radiotherapy. Front Oncol. 2019;9:156.

9. Sato H, Okonogi N, Nakano T. Rationale of combination of anti-PD-1/PD-L1 antibody therapy and radiotherapy for cancer treatment. Int J Clin Oncol. 2020;25:801-809.

10. Voli F, Valli E, Lerra L, Kimpton K, Saletta F, Giorgi FM, et al. Intratumoral Copper Modulates PD-L1 Expression and Influences Tumor Immune Evasion. Cancer research. 2020;80:4129-4144.

11. Wang X, Yang X, Zhang C, Wang Y, Cheng T, Duan L, et al. Tumor cell-intrinsic PD-1 receptor is a tumor suppressor and mediates resistance to PD-1 blockade therapy. Proc Natl Acad Sci U S A. 2020;117:6640-6650.

12. Azad A, Yin Lim S, D'Costa Z, Jones K, Diana A, Sansom OJ, et al. PD-L1 blockade enhances response of pancreatic ductal adenocarcinoma to radiotherapy. EMBO Mol Med. 2017;9:167-180.

13. Gong X, Li X, Jiang T, Xie H, Zhu Z, Zhou F, et al. Combined Radiotherapy and Anti-PD-L1 Antibody Synergistically Enhances Antitumor Effect in Non-Small Cell Lung Cancer. J Thorac Oncol. 2017;12:1085-1097.

14. Hartley GP, Chow L, Ammons DT, Wheat WH, Dow SW. Programmed Cell Death Ligand 1 (PD-L1) Signaling Regulates Macrophage Proliferation and Activation. Cancer Immunol Res. 2018;6:1260-1273.

15. Sumitomo R, Hirai T, Fujita M, Murakami H, Otake Y, Huang CL. PD-L1 expression on tumor-infiltrating immune cells is highly associated with M2 TAM and aggressive malignant potential in patients with resected non-small cell lung cancer. Lung Cancer. 2019;136:136-144.

16. Greten TF, Sangro B. Targets for immunotherapy of liver cancer. J Hepatol. 2017.

17. Salmaninejad A, Valilou SF, Shabgah AG, Aslani S, Alimardani M, Pasdar A, et al. PD-1/PD-L1 pathway: Basic biology and role in cancer immunotherapy. J Cell Physiol. 2019;234:16824-16837.

18. Scannell JW, Blanckley A, Boldon H, Warrington B. Diagnosing the decline in pharmaceutical R&D efficiency. Nat Rev Drug Discov. 2012;11:191-200.

19. Wu E. discovering new anticancer activities from old drugs. Curr Med Chem. 2013;20:4093-4094.

20. Nelson EA, Walker SR, Kepich A, Gashin LB, Hideshima T, Ikeda H, et al. Nifuroxazide inhibits survival of multiple myeloma cells by directly inhibiting STAT3. Blood. 2008;112:5095-5102.

21. Zhao T, Wei T, Guo J, Wang Y, Shi X, Guo S, et al. PD-1-siRNA delivered by attenuated Salmonella enhances the antimelanoma effect of pimozide. Cell Death Dis. 2019;10:164.

22. Boustani J, Lecoester B, Baude J, Latour C, Adotevi O, Mirjolet C, et al. Anti-PD-1/Anti-PD-L1 Drugs and Radiation Therapy: Combinations and Optimization Strategies. Cancers. 2021;13.

23. Yi M, Zheng X, Niu M, Zhu S, Ge H, Wu K. Combination strategies with PD-1/PD-L1 blockade: current advances and future directions. Mol Cancer. 2022;21:28.

24. Gong J, Le TQ, Massarelli E, Hendifar AE, Tuli R. Radiation therapy and PD-1/PD-L1 blockade: the clinical development of an evolving anticancer combination. J Immunother Cancer. 2018;6:46.

25. Zhang R, Yang Y, Dong W, Lin M, He J, Zhang X, et al. D-mannose facilitates immunotherapy and radiotherapy of triple-negative breast cancer via degradation of PD-L1. Proc Natl Acad Sci U S A. 2022;119.

26. Tong L, Li J, Li Q, Wang X, Medikonda R, Zhao T, et al. ACT001 reduces the expression of PD-L1 by inhibiting the phosphorylation of STAT3 in glioblastoma. Theranostics. 2020;10:5943-5956.

27. Cousin N, Cap S, Dihr M, Tacconi C, Detmar M, Dieterich LC. Lymphatic PD-L1 Expression Restricts Tumor-Specific CD8(+) T-cell Responses. Cancer Res. 2021;81:4133-4144.

28. Xiong H, Mittman S, Rodriguez R, Moskalenko M, Pacheco-Sanchez P, Yang Y, et al. Anti-PD-L1 Treatment Results in Functional Remodeling of the Macrophage Compartment. Cancer research. 2019;79:1493-1506.

29. Sun C, Mezzadra R, Schumacher TN. Regulation and Function of the PD-L1 Checkpoint. Immunity.

2018;48:434-452.

30. Dammeijer F, van Gulijk M, Mulder EE, Lukkes M, Klaase L, van den Bosch T, et al. The PD-1/PD-L1-Checkpoint Restrains T cell Immunity in Tumor-Draining Lymph Nodes. Cancer cell. 2020;38:685-700 e688.

31. Budimir N, Thomas GD, Dolina JS, Salek-Ardakani S. Reversing T-cell Exhaustion in Cancer: Lessons Learned from PD-1/PD-L1 Immune Checkpoint Blockade. Cancer Immunol Res. 2022;10:146-153.

32. Lhuillier C, Rudqvist NP, Elemento O, Formenti SC, Demaria S. Radiation therapy and anti-tumor immunity: exposing immunogenic mutations to the immune system. Genome Med. 2019;11:40.

33. Lan Y, Moustafa M, Knoll M, Xu C, Furkel J, Lazorchak A, et al. Simultaneous targeting of TGF-beta/PD-L1 synergizes with radiotherapy by reprogramming the tumor microenvironment to overcome immune evasion. Cancer Cell. 2021;39:1388-1403 e1310.

34. Ubil E, Caskey L, Holtzhausen A, Hunter D, Story C, Earp HS. Tumor-secreted Pros1 inhibits macrophage M1 polarization to reduce antitumor immune response. J Clin Invest. 2018;128:2356-2369.

35. Brown JM, Thomas R, Nagpal S, Recht L. Macrophage exclusion after radiation therapy (MERT): A new and effective way to increase the therapeutic ratio of radiotherapy. Radiother Oncol. 2020;144:159-164.

36. Yang Q, Guo N, Zhou Y, Chen J, Wei Q, Han M. The role of tumor-associated macrophages (TAMs) in tumor progression and relevant advance in targeted therapy. Acta Pharm Sin B. 2020;10:2156-2170.

Figure legends

Fig. 1 The effect of radiotherapy in combination with nifuroxazide on the proliferation, migration and apoptosis of Hep G2 cells. **A** The effect of the radiotherapy in combination with nifuroxazide on the viability of Hep G2 cells by CCK-8 assay. **B** The effect of the radiotherapy in combination with nifuroxazide on the proliferation of Hep G2 cells by cell clone formation assay. **C** The effect of the radiotherapy in combination with nifuroxazide on the migration of Hep G2 cells by Wound-Healing assay. **D** The effect of the radiotherapy in combination with nifuroxazide on the migration of Hep G2 cells by transwell assay. **E** The effect of the radiotherapy in combination with nifuroxazide on the apoptosis of Hep G2 cells by flow cytometry assay. The data were presented as mean ± SD (n=3). Compared with the control group, *P<0.05; compared with "4Gy" group, #P<0.05.

Fig. 2 The effect of radiotherapy in combination with nifuroxazide on the expressions of tumor-associated proteins in cells. After radiotherapy, Hep G2 cells were treated with nifuroxazide at the different dose. At 24 h or 48 h after being incubated, the expression of tumor-associated proteins was detected by Western blot. **A-E** The expression of Stat3, p-Stat3, PCNA, Ki67 and cyclin D1 related with cell proliferation was analyzed by Western blot. **F-N** The expression of cytochrome C, pro-caspase 3, c-caspase 3, pro-caspase 9, c-caspase 9, Bax, Bcl-2, PARP and c-PARP related with cell apoptosis was analyzed by Western blot. The data are presented as mean ± SD (n=3). Compared with the control group, *P<0.05; compared with "4Gy" group, #P<0.05.

Fig. 3 The effects of radiotherapy in combination with nifuroxazide on tumor growth and survival of tumor-bearing mice. At 7 days after establishing the tumor model, the mice are received distinct treatments. **A** Treatment scheme of different methods. **B** Tumor pictures and tumor weight of tumor-bearing mice under different treatments are measured for statistical analysis. **C** The tumor volume changes of tumor-bearing mice under different treatments. **D** The survival of tumor bearing mice under different treatments. **E** Pathological pictures of tumor-bearing mice under different treatments. **F** Statistical analysis of pathological score. The data are presented as mean ± SD (n=3). Compared with the PBS group, *P<0.05; compared with the radiotherapy group, $$P$<0.05; compared with nifuroxazide group, #P<0.05.

Fig. 4 The effects of radiotherapy in combination with nifuroxazide on the cell proliferation or apoptosis in tumor tissues. **A-C** The expression of Ki6, PCNA or c-caspase-3 in tumor tissues is detected by immunohistochemistry. **D** The cell apoptosis on tumor tissues is detected by TUNEL assay.

E-N The protein expression of Stat3, p-Stat3, Ki67, PCNA, cyclin D1, cytochrome C, Bcl-2, Bax, pro-caspase 3 and c-caspase 3 in tumor tissues is detected by Western blot. The data are presented as mean ± SD (n=3). Compared with the PBS group, *P<0.05; compared with the radiotherapy group, #P<0.05; compared with the nifuroxazide group, $$P$<0.05.

Fig. 5 The effects of radiotherapy in combination with nifuroxazide on the infiltration of immune cells in tumor tissues. **A-C** Different isoforms of T lymphocytes infiltration in tumor tissues detected by immunofluorescence assay. **D** M1 macrophage infiltration in tumor tissues detected by immunofluorescence assay. **E** Statistical analysis about Semi quantitative of Image A-D. **F-I** The protein expression of CD4, CD8, CD86 and Granzyme in tumor tissues is detected by Western blot. The data are presented as mean ± SD (n=3). Compared with the PBS group, *P<0.05; compared with the radiotherapy group, #P<0.05; compared with the nifuroxazide group, $$P$<0.05.

Fig. 6 The effect of radiotherapy in combination with nifuroxazide on the ratios of immune cells in spleens. The ratios of immune cells in the spleens of tumor-bearing mice were detected by flow cytometry. The data are presented as mean ± SD (n=3). Compared with the PBS group, *P<0.05; compared with the radiotherapy group, #P<0.05; compared with the nifuroxazide group, $$P$<0.05.

Fig. 7 Nifuroxazide in combination with the radiotherapy significantly increase the degradation of pd-l1 through ubiquitination proteasome pathway. **A** The expression of PD-L1 in cells combined treatment with radiotherapy and nifuroxazide is detected by Western blot. **B** The mRNA level of PD-L1 in cells is detected by PCR. **C-E** The effect of the radiotherapy combined with nifuroxazide on PD-L1 degradation through ubiquitination-proteasome pathway. **F** The schematic diagram of the mechanism that nifuroxazide degraded PD-L1 through ubiquitination-proteasome pathway. The data are presented as mean ± SD (n=3). Compared with “0” group, *P<0.05; compared with “4Gy” group, #P<0.05.

Fig. 8 The effect of radiotherapy in combination with nifuroxazide on the expression of pd-l1 in tumor tissues. **A** PD-L1 expression in tumor tissues of HCC patients treated with radiotherapy are detected by immunofluorescence. **B** PD-L1 expression in tumor tissues of mice combined treatment with radiotherapy and nifuroxazide is detected by immunofluorescence. **C-D** The expression of PD-L1 or GSK3β in tumor tissues of mice combined treatment with radiotherapy and nifuroxazide is detected by Western blot. The data were expressed as mean ± SD (n=3). Compared with the before-radiotherapy samples, **** P<0.0001; compared with the PBS group, *P<0.05; compared with the radiotherapy group, #P<0.05; compared with the nifuroxazide group, $$P$<0.05.

Fig. 9 The synergistic antitumor mechanism of radiotherapy in combination with nifuroxazide in tumor-bearing mice. NK cell: natural killer cell. Treg: regulatory T cells. TAM: tumor-associated macrophage. $CD8^+$ CTL: $CD8^+$ cytotoxic lymphocyte.

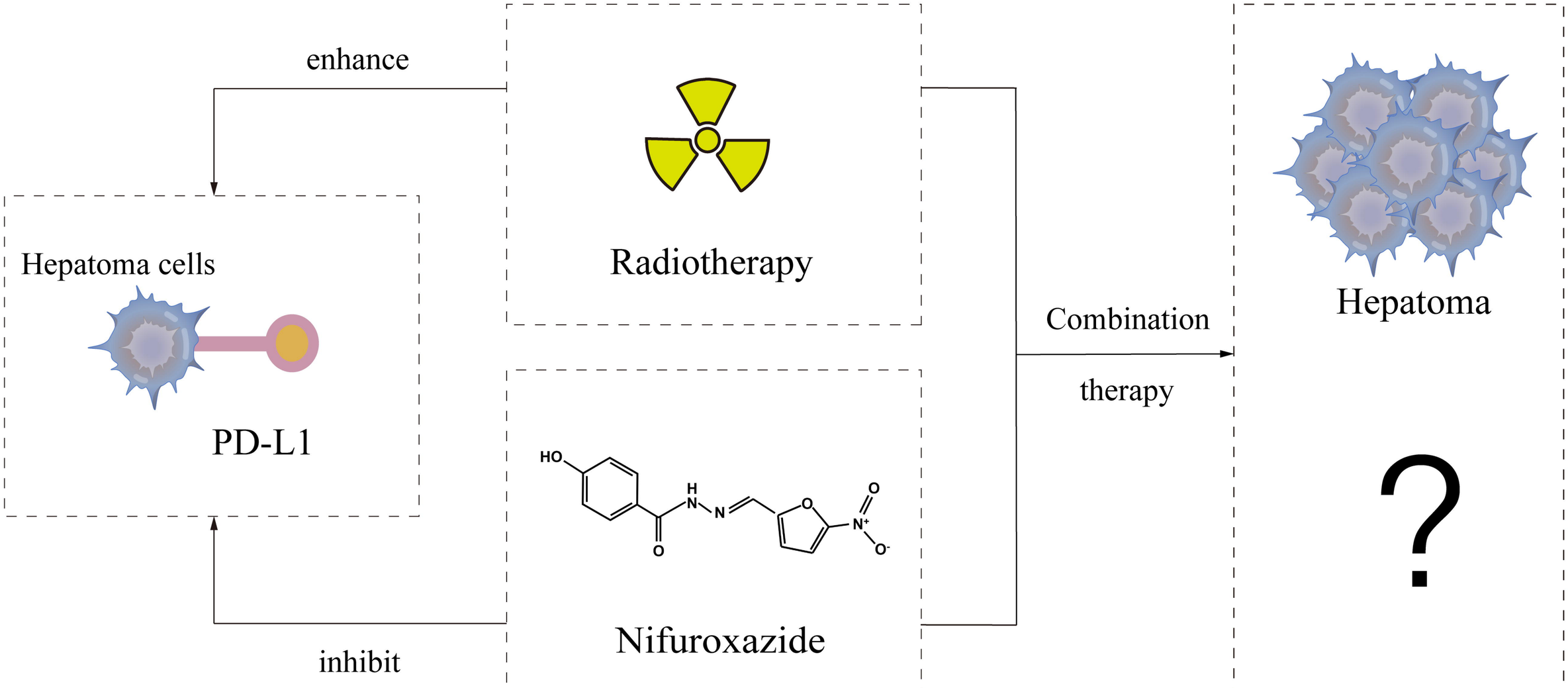
enhance
Hepatoma cells
PD-L1
Radiotherapy
HO
H
N
N
O
O
O
N+
O-
Nifuroxazide
inhibit
Combination
therapy
Hepatoma
?

Figure 1

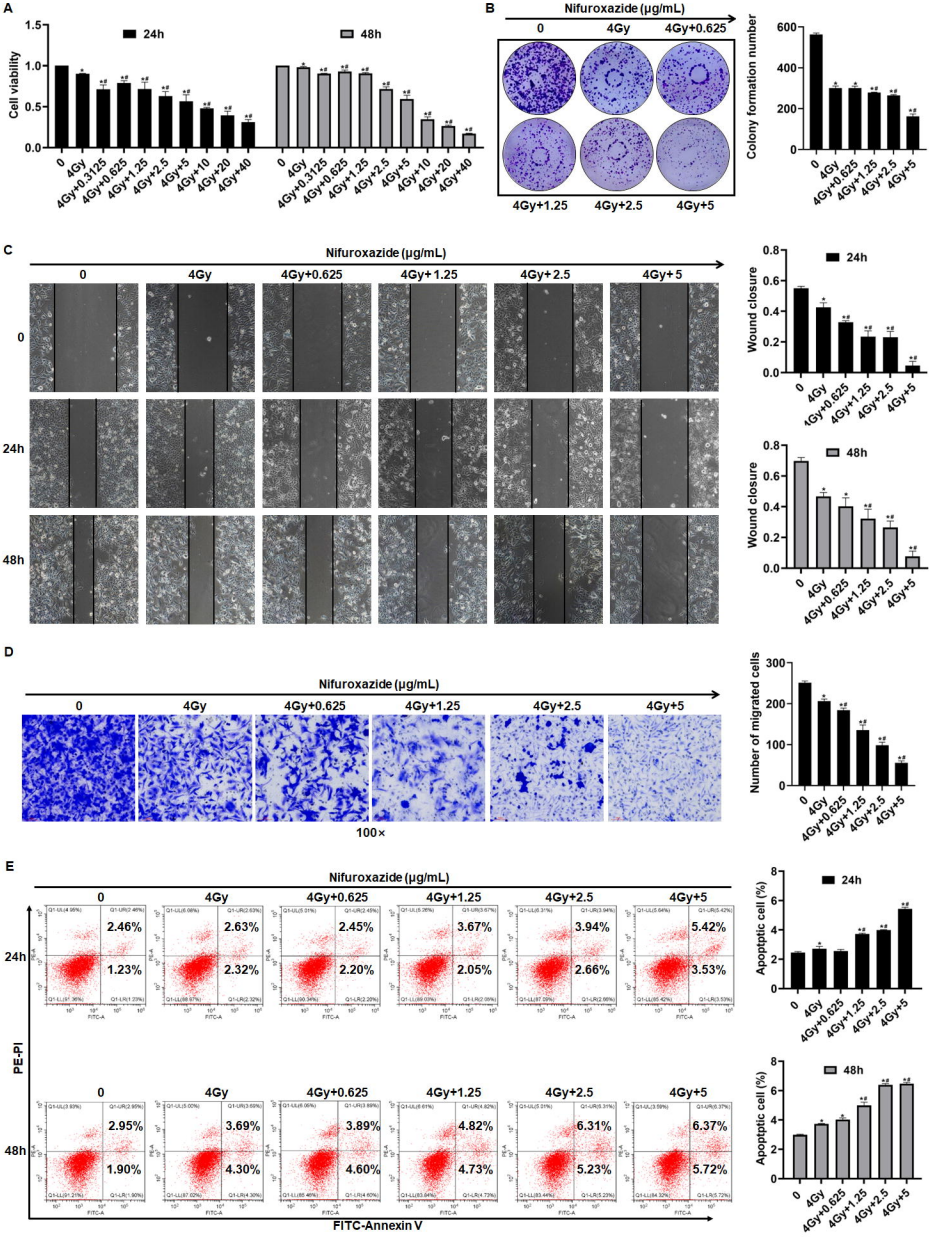
A
24h
48h
Cell viability
0
4Gy
4Gy+0.3125
4Gy+0.625
4Gy+1.25
4Gy+2.5
4Gy+5
4Gy+10
4Gy+20
4Gy+40
B
Nifuroxazide (μg/mL)
0
4Gy
4Gy+0.625
4Gy+1.25
4Gy+2.5
4Gy+5
Colony formation number
C
Nifuroxazide (μg/mL)
0
4Gy
4Gy+0.625
4Gy+1.25
4Gy+2.5
4Gy+5
24h
48h
Wound closure
D
Nifuroxazide (μg/mL)
0
4Gy
4Gy+0.625
4Gy+1.25
4Gy+2.5
4Gy+5
100×
Number of migrated cells
E
Nifuroxazide (μg/mL)
0
4Gy
4Gy+0.625
4Gy+1.25
4Gy+2.5
4Gy+5
24h
48h
PE-PI
FITC-Annexin V
Apoptptic cell (%)

Figure 2

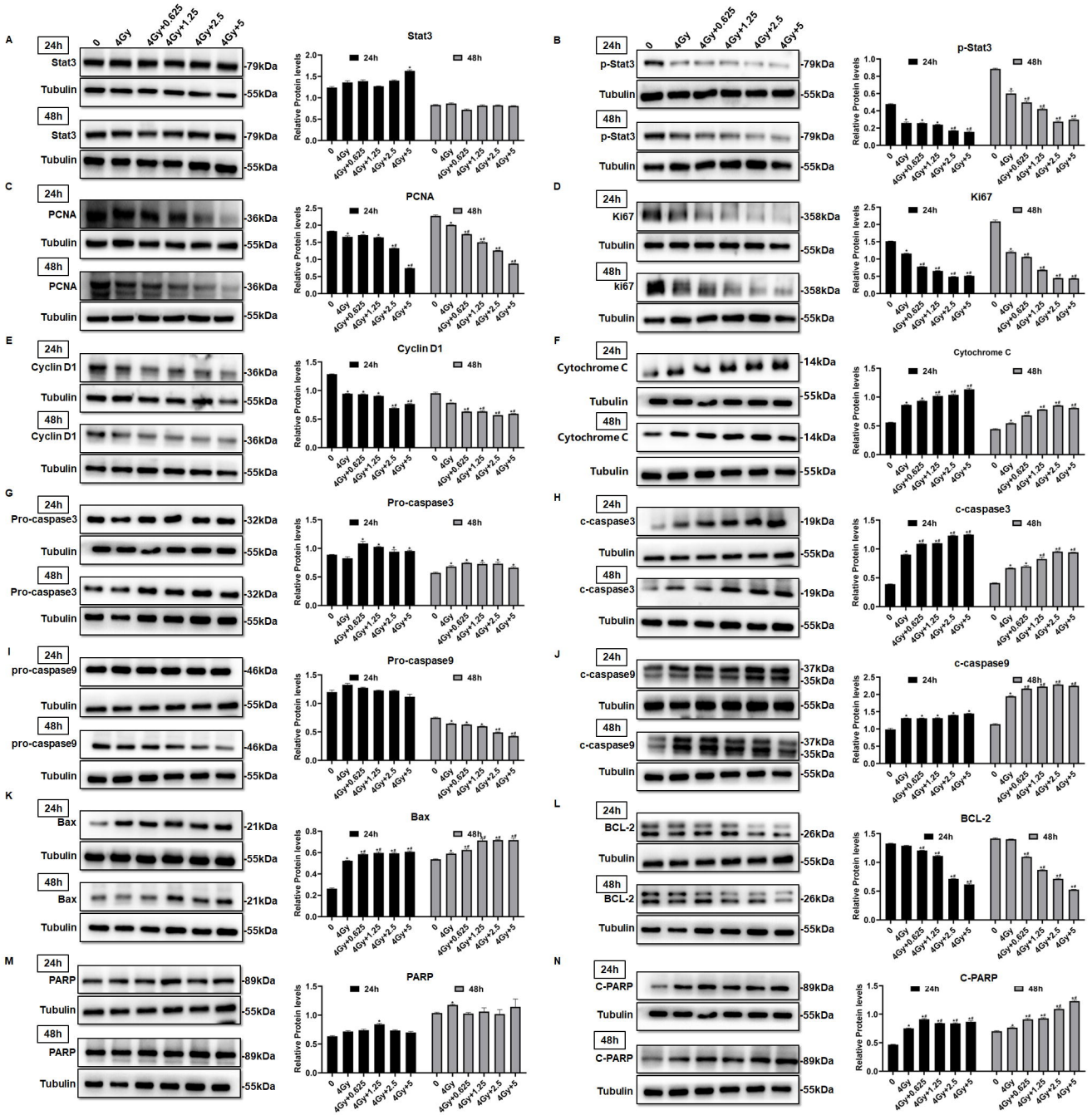
A
Stat3
B
p-Stat3
C
PCNA
D
Ki67
E
Cyclin D1
F
Cytochrome C
G
Pro-caspase3
H
c-caspase3
I
pro-caspase9
J
c-caspase9
K
Bax
L
BCL-2
M
PARP
N
C-PARP
24h
48h
Tubulin
0
4Gy
4Gy+0.625
4Gy+1.25
4Gy+2.5
4Gy+5
Relative Protein levels

Figure 3

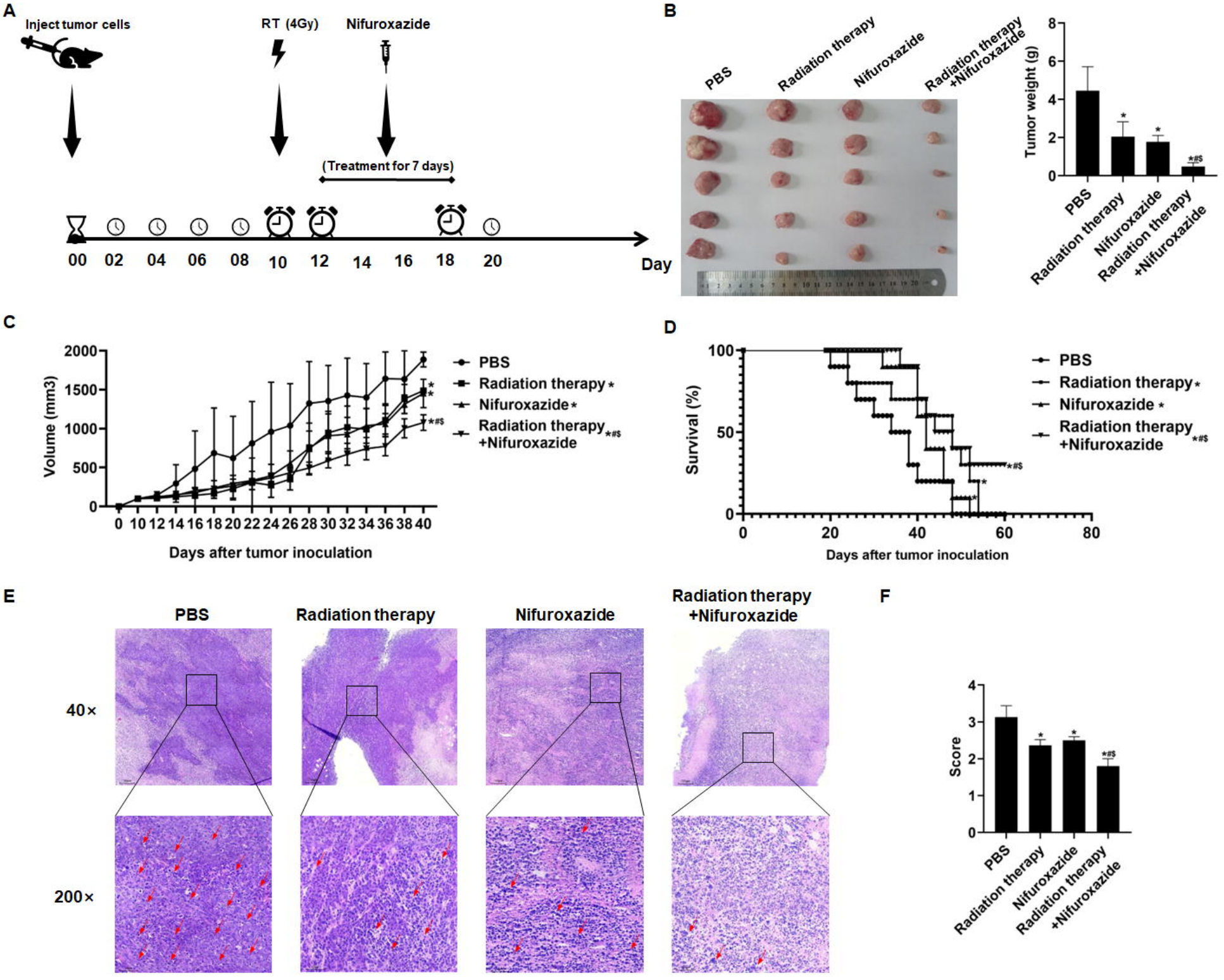
A
Inject tumor cells
RT (4Gy)
Nifuroxazide
(Treatment for 7 days)
00 02 04 06 08 10 12 14 16 18 20
Day
B
PBS
Radiation therapy
Nifuroxazide
Radiation therapy +Nifuroxazide
Tumor weight (g)
C
Volume (mm3)
Days after tumor inoculation
PBS
Radiation therapy*
Nifuroxazide*
Radiation therapy +Nifuroxazide*#$
D
Survival (%)
Days after tumor inoculation
PBS
Radiation therapy*
Nifuroxazide*
Radiation therapy +Nifuroxazide*#$
E
PBS
Radiation therapy
Nifuroxazide
Radiation therapy +Nifuroxazide
40×
200×
F
Score

Figure 4

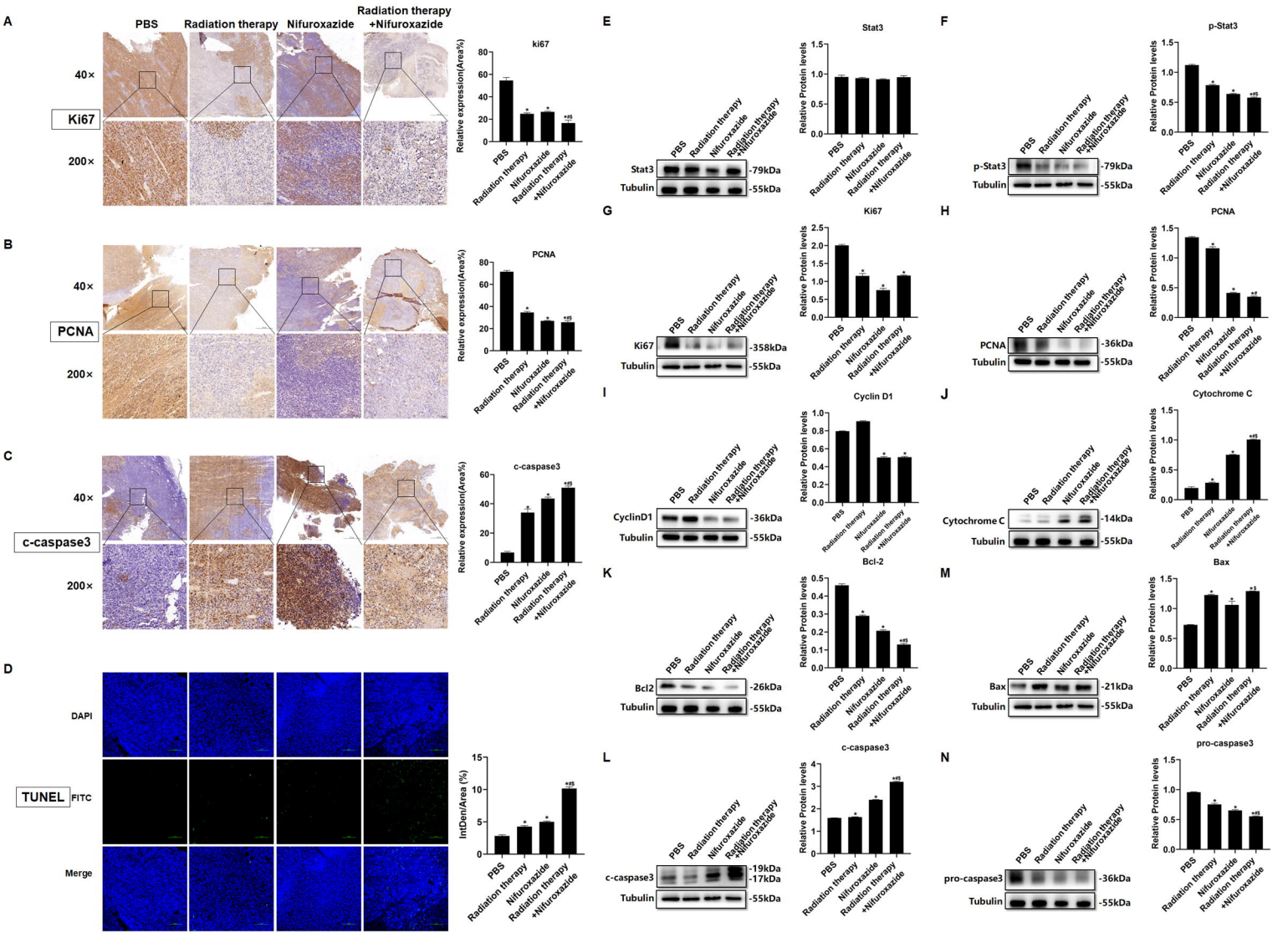
A
PBS
Radiation therapy
Nifuroxazide
Radiation therapy +Nifuroxazide
40×
Ki67
200×
ki67
Relative expression(Area%)
B
PCNA
c-caspase3
C
D
DAPI
TUNEL FITC
Merge
IntDen/Area (%)
E
Stat3
Tubulin
-79kDa
-55kDa
Relative Protein levels
F
p-Stat3
G
Ki67
-358kDa
H
PCNA
-36kDa
I
Cyclin D1
CyclinD1
J
Cytochrome C
-14kDa
K
Bcl-2
Bcl2
-26kDa
M
Bax
-21kDa
L
c-caspase3
-19kDa
-17kDa
N
pro-caspase3
PBS
Radiation therapy
Nifuroxazide
Radiation therapy +Nifuroxazide

Figure 5

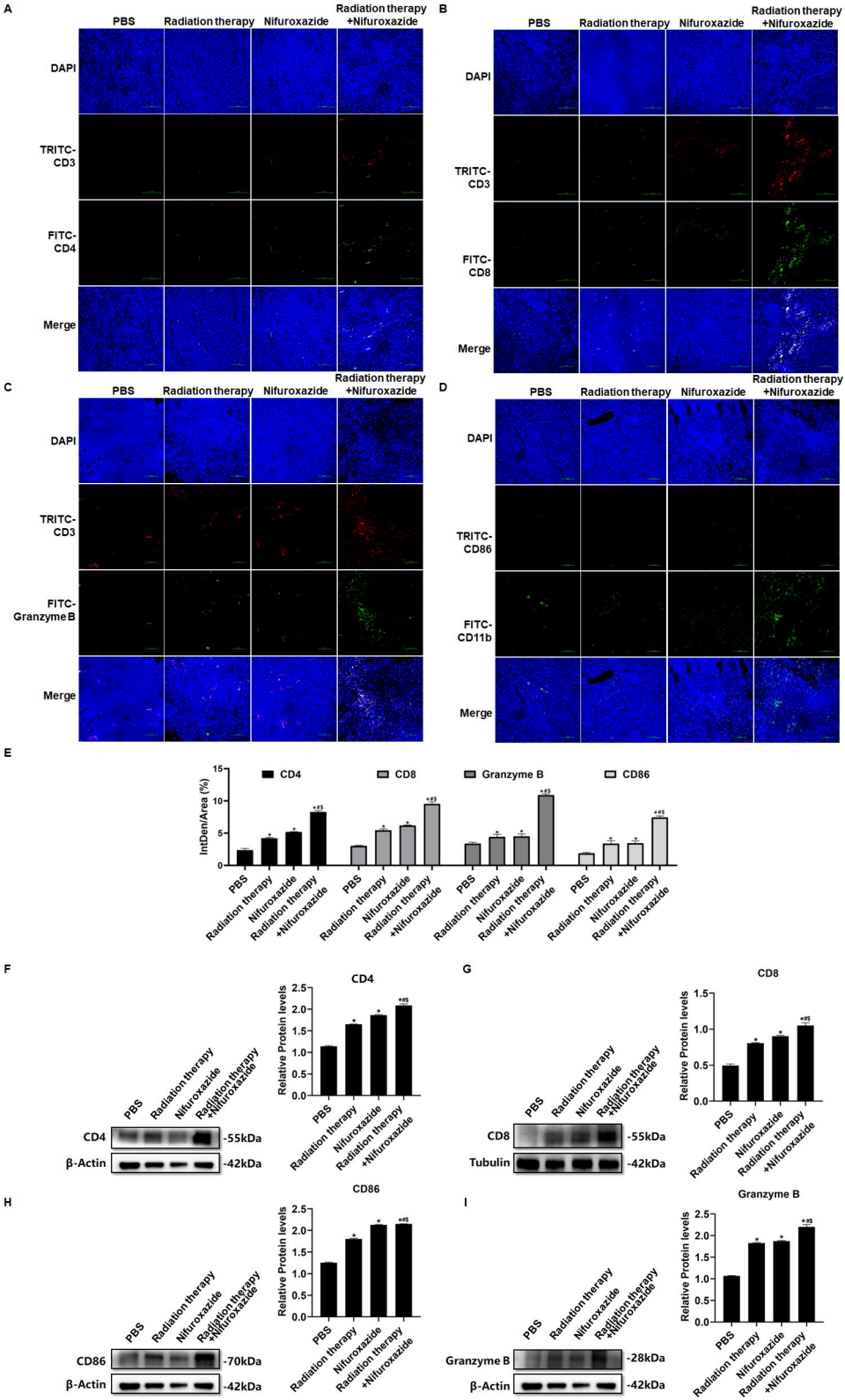
A
PBS
Radiation therapy
Nifuroxazide
Radiation therapy +Nifuroxazide
DAPI
TRITC-CD3
FITC-CD4
Merge
B
DAPI
TRITC-CD3
FITC-CD8
Merge
C
DAPI
TRITC-CD3
FITC-Granzyme B
Merge
D
DAPI
TRITC-CD86
FITC-CD11b
Merge
E
CD4
CD8
Granzyme B
CD86
IntDen/Area (%)
F
CD4
Relative Protein levels
CD4
β-Actin
-55kDa
-42kDa
G
CD8
Tubulin
-55kDa
-42kDa
H
CD86
CD86
β-Actin
-70kDa
-42kDa
I
Granzyme B
Granzyme B
β-Actin
-28kDa
-42kDa

Figure 6

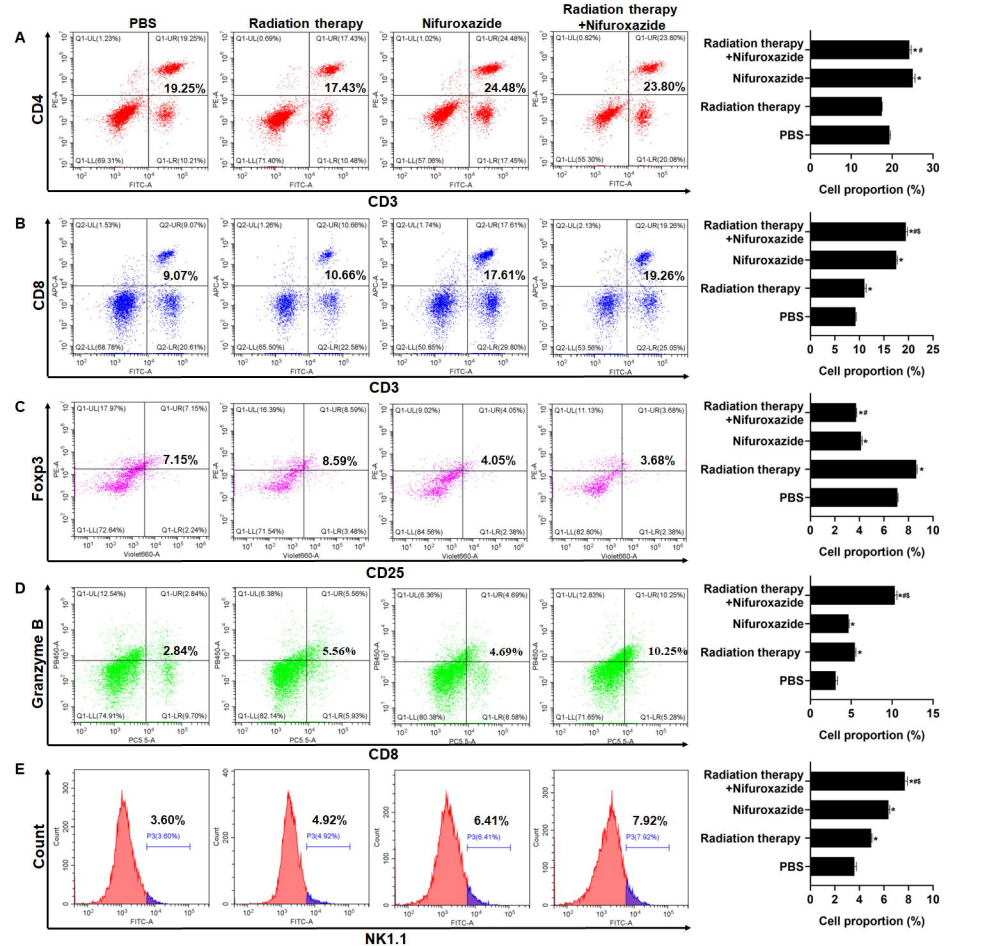
PBS
Radiation therapy
Nifuroxazide
Radiation therapy +Nifuroxazide
A
CD4
CD3
19.25%
17.43%
24.48%
23.80%
B
CD8
CD3
9.07%
10.66%
17.61%
19.26%
C
Foxp3
CD25
7.15%
8.59%
4.05%
3.68%
D
Granzyme B
CD8
2.84%
5.56%
4.69%
10.25%
E
Count
NK1.1
3.60%
4.92%
6.41%
7.92%
Radiation therapy +Nifuroxazide
Nifuroxazide
Radiation therapy
PBS
Cell proportion (%)

Figure 7

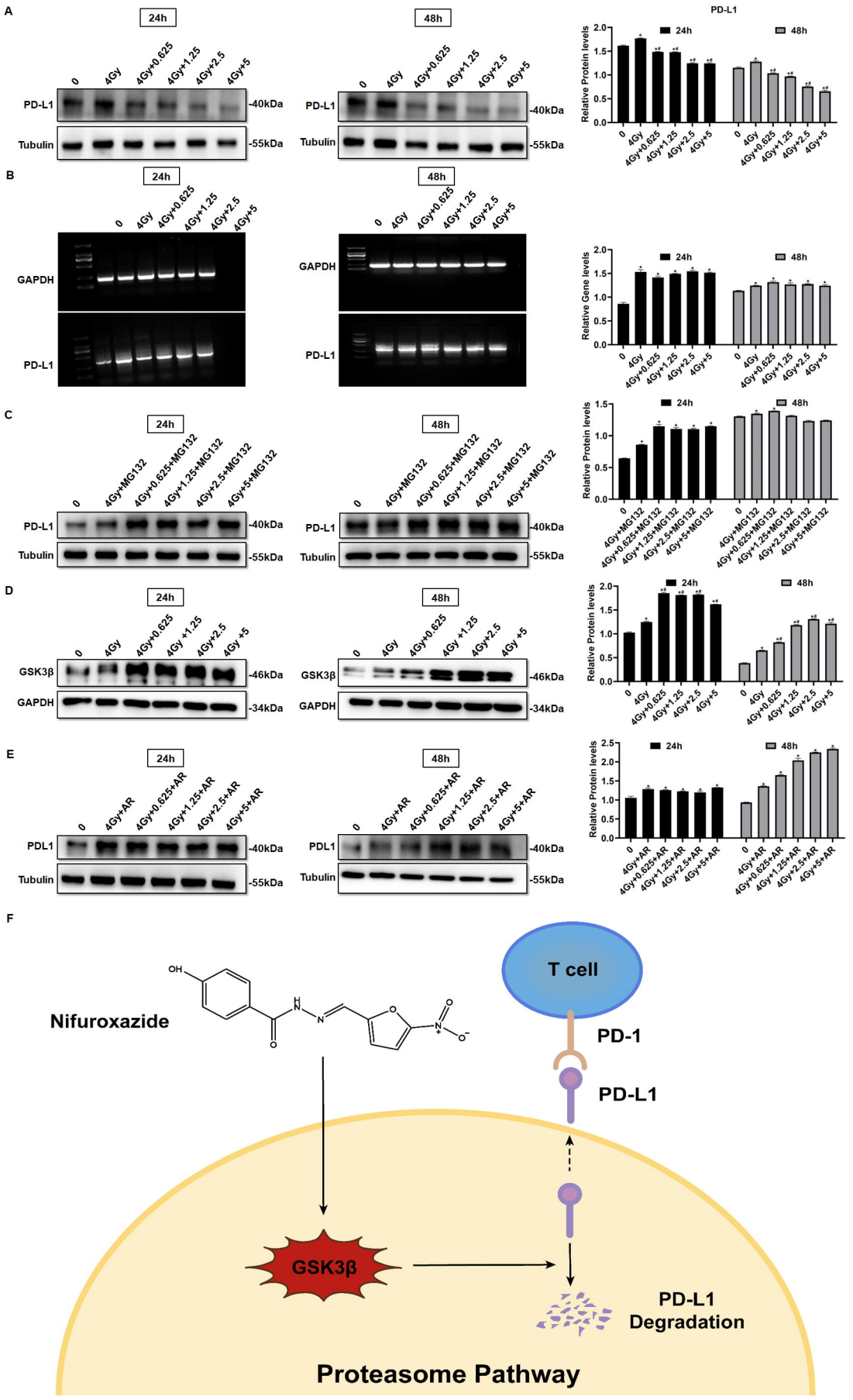
A
24h
48h
0
4Gy
4Gy+0.625
4Gy+1.25
4Gy+2.5
4Gy+5
PD-L1
Tubulin
-40kDa
-55kDa
Relative Protein levels
B
GAPDH
Relative Gene levels
C
4Gy+MG132
4Gy+0.625+MG132
4Gy+1.25+MG132
4Gy+2.5+MG132
4Gy+5+MG132
D
GSK3β
-46kDa
-34kDa
E
4Gy+AR
4Gy+0.625+AR
4Gy+1.25+AR
4Gy+2.5+AR
4Gy+5+AR
PDL1
F
Nifuroxazide
T cell
PD-1
PD-L1
GSK3β
PD-L1
Degradation
Proteasome Pathway

Figure 8

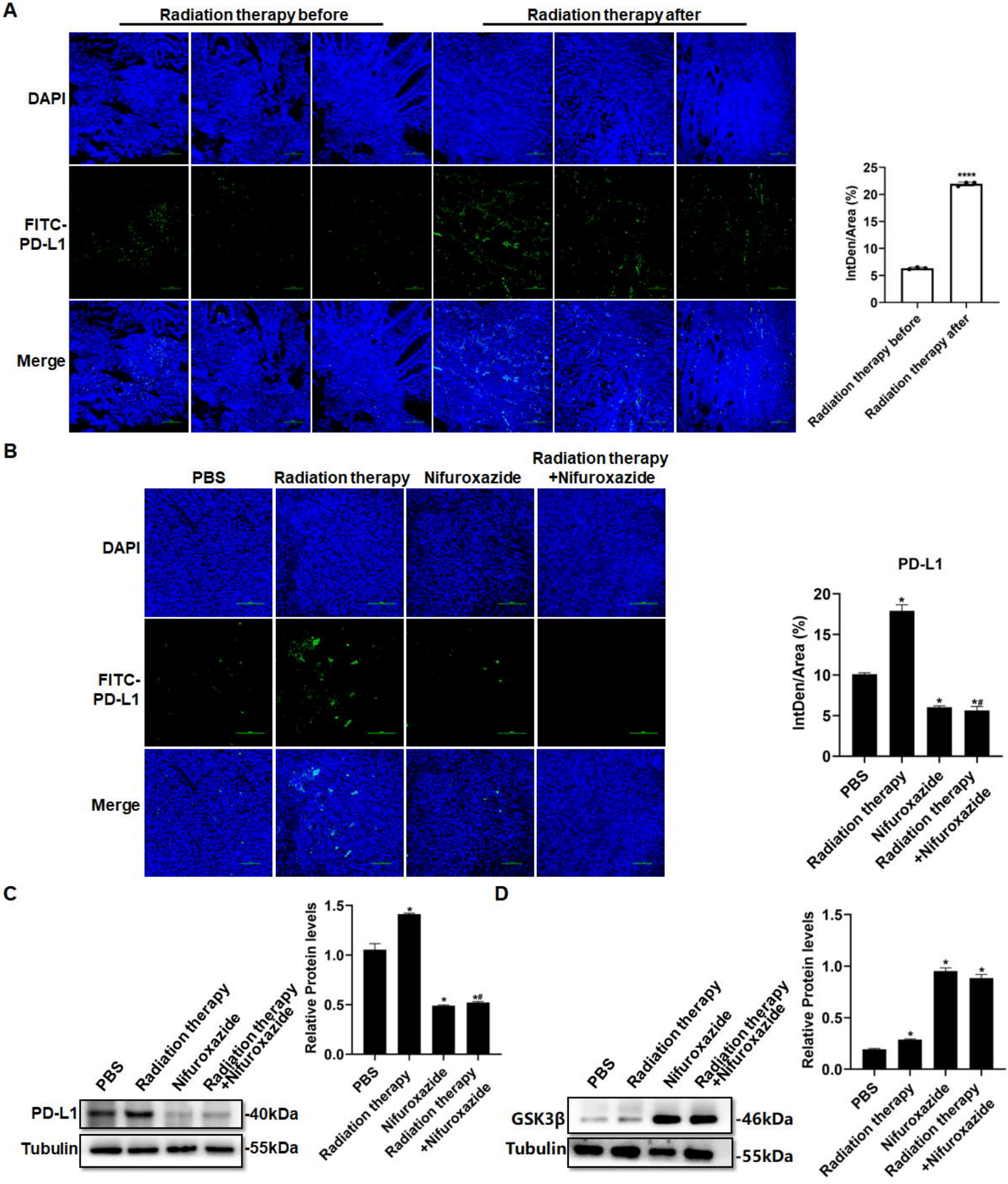
A
Radiation therapy before
Radiation therapy after
DAPI
FITC-PD-L1
Merge
IntDen/Area (%)
****
Radiation therapy before
Radiation therapy after
B
PBS
Radiation therapy
Nifuroxazide
Radiation therapy +Nifuroxazide
DAPI
FITC-PD-L1
Merge
PD-L1
IntDen/Area (%)
PBS
Radiation therapy
Nifuroxazide
Radiation therapy +Nifuroxazide
C
PBS
Radiation therapy
Nifuroxazide
Radiation therapy +Nifuroxazide
PD-L1
-40kDa
Tubulin
-55kDa
Relative Protein levels
D
PBS
Radiation therapy
Nifuroxazide
Radiation therapy +Nifuroxazide
GSK3β
-46kDa
Tubulin
-55kDa
Relative Protein levels

Figure 9

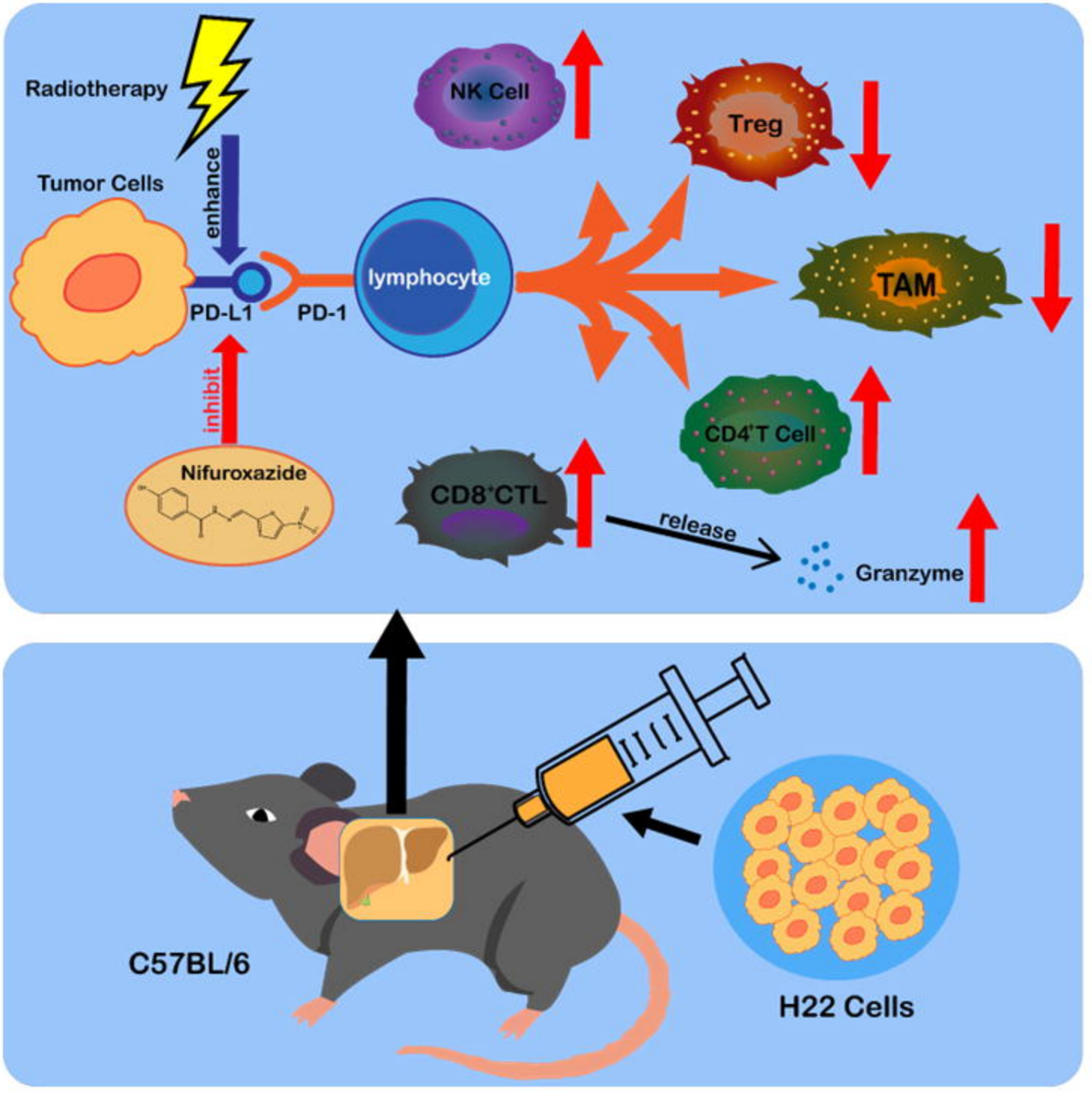
Radiotherapy
Tumor Cells
enhance
PD-L1
PD-1
lymphocyte
NK Cell
Treg
TAM
CD4⁺T Cell
CD8⁺CTL
release
Granzyme
inhibit
Nifuroxazide
C57BL/6
H22 Cells